

Missing momentum of charged particles at 900 MeV/c and
resistive wire length scaling

Matthias Heinzelmann

University of Zürich

Abstract

In-flight data at various beam momenta shows a substantial discrepancy between incoming \bar{p} momentum and measured total z-momentum. The resistive wire length of the JDC used in the reconstruction of charged tracks has to be scaled by 6 % in order to get correct momenta.

In-flight data at various beam momenta shows a substantial discrepancy between incoming \bar{p} momentum and measured total z-momentum. The total z-momentum of three data samples at 900 MeV ($\pi^+\pi^-$, $\pi^+\pi^-\pi^0$ and $K^+K^-\pi^0$) for different scaling factors α (with $p_z^{total} = \alpha \times p_z^{charged} + p_z^{neutral}$) is shown in figure 1. As different fractions of the total momentum is covered by the charged tracks the dependence of α for each sample is different. Only when a scaling factor of $\alpha = 1.06$ is applied all three data samples show a consistent total z-momentum (as expected at about 900 MeV).

The reconstruction of the tracks is done by fitting a helix through the corresponding hits in the JDC with λ the opening angle of the helix perpendicular to the beam axis. A scaling of the z-momentum corresponds to an identical scaling of $\tan(\lambda)$ because p_z is given by

$$p_z = p_{xy} \cdot \tan(\lambda). \quad (1)$$

As the z-position of the hits in the JDC is calculated through charge division, a $\tan(\lambda)$ scaling can be caused by a wrong resistive wire length used for the reconstruction (cf. figure 2). Therefore, a scaling factor for the z-momentum is identical with a scaling factor for the resistive wire length.

A possible check of this scaling factor uses the information of the PEDs matched to the charged tracks, connecting JDC and Barrel as two independent detector components. The intersection point of the track with the Barrel should coincide with the position of the corresponding matched PED. Figures 3 and 4 show the differences in CB-coordinates between the entry point of the track and the PED position for 900 MeV data. The x and y positions coincide well whereas a significant difference in the z coordinate exists. A possible parametrisation of the difference in z is

$$\Delta z = (\alpha \times z_{JDC} + z_0) - z_{PED}, \quad (2)$$

where α corresponds to a scaling of the resistive wire length of the JDC and z_0 to an offset between JDC and Barrel. A scan in α and z_0 was performed with different slices and for every pair of α and z_0 the position of the Δz peak (cf. figure 4) was obtained. The slices were necessary because of the different impact of the scaling factor on tracks in the front or back half of the JDC and the different numbers of forward and backward tracks. The slices were defined in z_{PED} in steps of 5 cm from -25 cm to $+25$ cm (i.e. 0 cm $< z_{PED} < 5$ cm). The result is shown in figure 6 as

$$\sum_{slices} (\Delta z)^2, \quad (3)$$

summed over all 10 slices. There is a clear minimum at $\alpha = 1.06$ and $z_0 = 0.5$.

Another possibility is the FWHM of the distance

$$r = \sqrt{(\Delta x)^2 + (\Delta y)^2 + (\Delta z)^2} \quad (4)$$

between the entry point of the track into the barrel and the matched PED (figure 5) in dependence of α and z_0 . The result of this scan is shown in figure 7. The plot shows a minimum near $\alpha = 1.06$ and $z_0 = 0.5$, too.

A further check is the position of the very narrow peak of the $\Phi(1020)$ in $K^+K^-\pi^0$. Figures 8 and 9 show the K^+K^- invariant mass around 1000 MeV for data taken at 900 MeV. Without any corrections (cf. figure 8) the $\Phi(1020)$ - peak is slightly too low whereas for a scaling factor of $\alpha = 1.06$ the peak is nicely centered at 1019 MeV (the line corresponds to $m_\phi = 1019.4$ MeV).

Figure 10 shows the result of a scan of α and z_0 for Δz using at rest data from June 1994 ($K^\pm\pi^\mp K_L$, for technical reasons only two slices ($z_{PED} > 0$ and $z_{PED} < 0$) were done). The minimum lies near $\alpha = 1.06$.

In-flight data at 900 MeV require a scaling of the resistive wire length of $\alpha = 1.06$ in order to be consistent with the \bar{p} beam momentum. Without this scaling different data samples show different total z-momentum. This scaling factor of 1.06 is not inconsistent with at rest data.

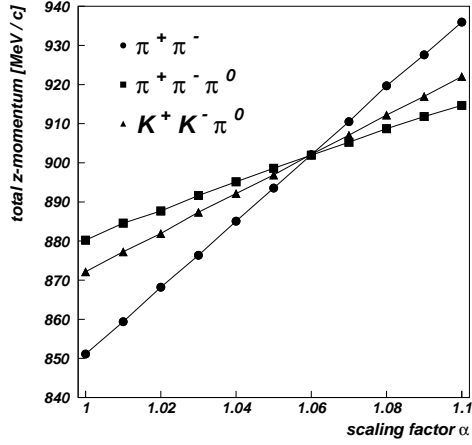


Figure 1: Total z-momentum of $\pi^+\pi^-$, $\pi^+\pi^-\pi^0$ and $K^+K^-\pi^0$ in dependence of the scaling of the charged z-momenta.

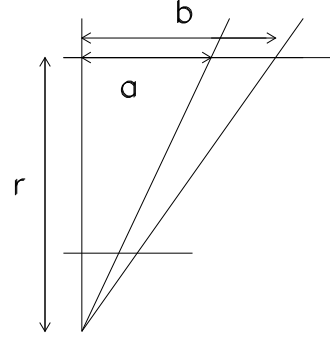


Figure 2: The scaling of $\tan(\lambda)$ corresponds to a wire length scaling with the same factor: $\alpha \times \tan(\lambda) = \alpha \times \frac{a}{r} = \frac{b}{r}$

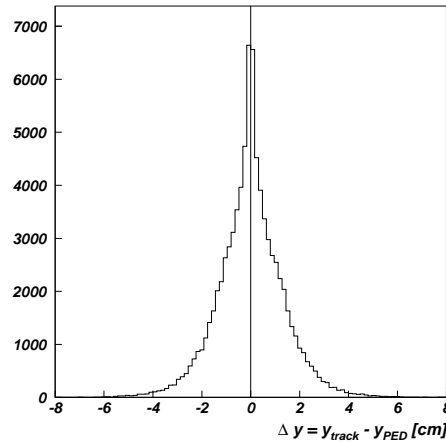
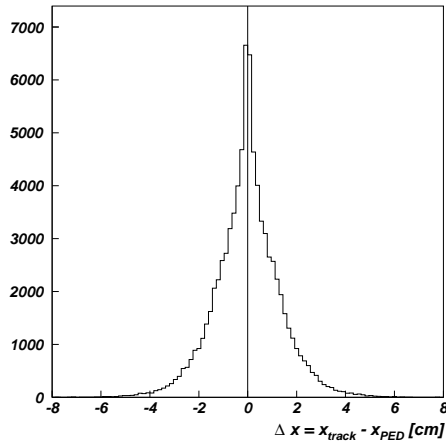


Figure 3: Difference in CB-coordinates (x,y) between the entry point of a track and the position of the matched PED.

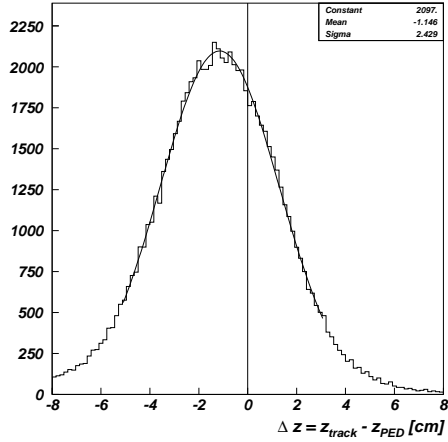


Figure 4: Difference in CB-coordinate (z) between the entry point of a track and the position of the matched PED.

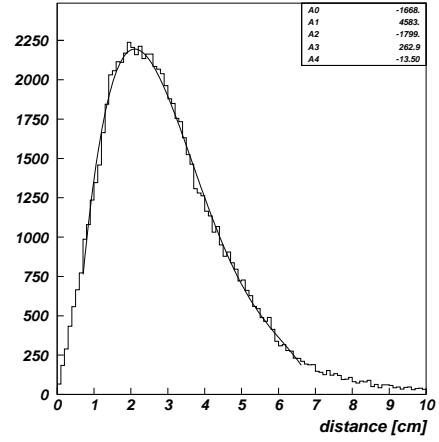


Figure 5: Distance between track and matched PED.

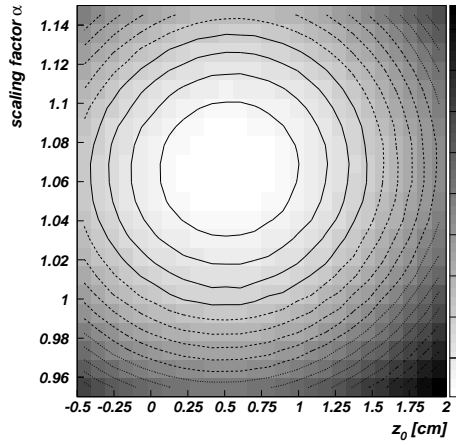


Figure 6: Sum of $(\Delta z)^2$ for all slices in dependence of α and z_0 (900 MeV data).

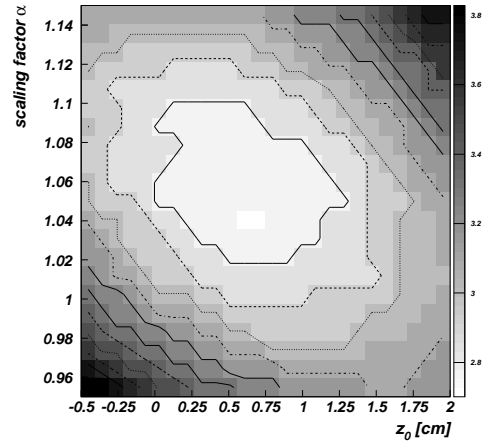


Figure 7: FWHM of the distance of the entry point of the track to the matched PED in dependence of α and z_0 (900 MeV data).

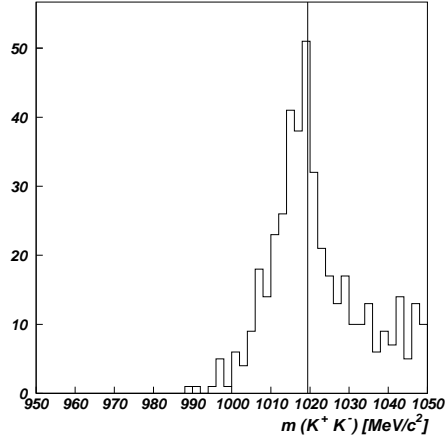


Figure 8: K^+K^- invariant mass for $K^+K^-\pi^0$ at 900 MeV and no correction applied. The peak of the $\Phi(1020)$ is slightly below 1019.4 MeV.

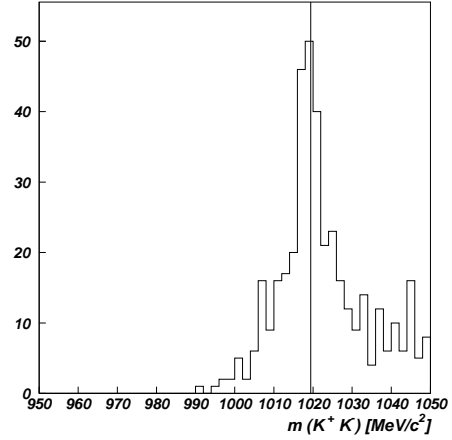


Figure 9: The same peak when a scaling factor of $\alpha = 1.06$ was applied. The invariant mass peaks at the expected value.

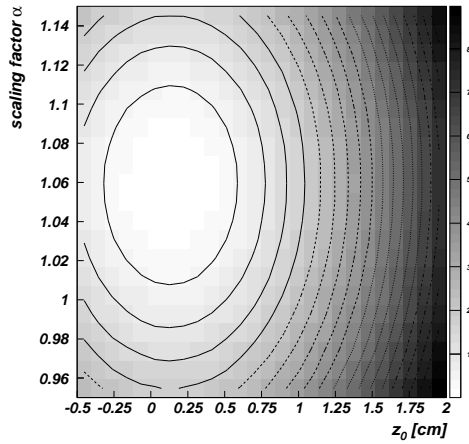


Figure 10: Sum of $(\Delta z)^2$ for all slices in dependence of α and z_0 (at rest data).